



# Identification of potential inhibitors of *Mycobacterium tuberculosis* shikimate kinase: molecular docking, in silico toxicity and in vitro experiments

Talita Freitas de Freitas<sup>1,2</sup> · Candida Deves Roth<sup>1</sup> · Bruno Lopes Abbadi<sup>1</sup> · Fernanda Souza Macchi Hopf<sup>1,3</sup> · Marcia Alberton Perelló<sup>1</sup> · Alexia de Matos Czczot<sup>1,2</sup> · Eduardo Vieira de Souza<sup>1,3</sup> · Ana Flávia Borsoi<sup>1,2</sup> · Pablo Machado<sup>1,2,3</sup> · Cristiano Valim Bizarro<sup>1,3</sup> · Luiz Augusto Basso<sup>1,2,3</sup> · Luis Fernando Saraiva Macedo Timmers<sup>1,4,5,6</sup>

Received: 28 June 2022 / Accepted: 9 December 2022 / Published online: 22 December 2022  
© The Author(s), under exclusive licence to Springer Nature Switzerland AG 2022

## Abstract

Tuberculosis (TB) is one of the main causes of death from a single pathological agent, *Mycobacterium tuberculosis* (*Mtb*). In addition, the emergence of drug-resistant TB strains has exacerbated even further the treatment outcome of TB patients. It is thus needed the search for new therapeutic strategies to improve the current treatment and to circumvent the resistance mechanisms of *Mtb*. The shikimate kinase (SK) is the fifth enzyme of the shikimate pathway, which is essential for the survival of *Mtb*. The shikimate pathway is absent in humans, thereby indicating SK as an attractive target for the development of anti-TB drugs. In this work, a combination of in silico and in vitro techniques was used to identify potential inhibitors for SK from *Mtb* (*MtSK*). All compounds of our in-house database (Centro de Pesquisas em Biologia Molecular e Funcional, CPBMF) were submitted to in silico toxicity analysis to evaluate the risk of hepatotoxicity. Docking experiments were performed to identify the potential inhibitors of *MtSK* according to the predicted binding energy. In vitro inhibitory activity of *MtSK*-catalyzed chemical reaction at a single compound concentration was assessed. Minimum inhibitory concentration values for in vitro growth of pan-sensitive *Mtb* H37Rv strain were also determined. The mixed approach implemented in this work was able to identify five compounds that inhibit both *MtSK* and the in vitro growth of *Mtb*.

**Keywords** *Mycobacterium tuberculosis* · Shikimate kinase · Docking · AutoDock Vina · PyRx · pkCSM

## Introduction

From 2020, with the emergence of COVID-19, tuberculosis (TB) became the second leading cause of death worldwide from a single pathological agent, *Mycobacterium tuberculosis* (*Mtb*). The COVID-19 pandemic has had a negative impact on TB: for the first time in 10 years, there was an increase in the number of TB deaths due to the lack of access to both diagnosis and treatment [1]. In addition, the emergence of TB drug-resistant strains makes the search for less toxic drugs and shorter TB treatment urgent efforts to be pursued. The shikimate pathway, which is present in bacteria, fungi and plants, but absent in humans, is interesting

for the development of new anti-TB therapeutic agents with likely reduced risk of toxicity to the host. In 2002, Parish and collaborators performed the deletion of the *aroK* gene that encodes the shikimate kinase (SK) enzyme in *Mtb* (*MtSK*), proving the essentiality of this gene product for the viability of the bacillus [2, 3].

The SK enzyme catalyzes the fifth step of the shikimate pathway, which is the phosphorylation of shikimate (SKM), using ATP as a phosphate donor to form shikimate-3-phosphate (S3P) and adenosine diphosphate (ADP). SK is a member of the Nucleoside Monophosphate Kinase (NMP) family, an important group of enzymes that catalyze the reversible transfer of a phosphate of a nucleoside triphosphate to a specific nucleoside diphosphate. NMP kinases undergo to major conformational changes during catalysis [4, 5]. The determination of SKM binding pocket in a crystallographic structure of SK complexed with ADP:SKM and the structure ATP:shikimate 3-phosphotransferase allowed

✉ Luis Fernando Saraiva Macedo Timmers  
luis.timmers@univates.br

Extended author information available on the last page of the article

a better understanding of the intermolecular interactions between ligands and the enzyme [4–7].

Computational tools can be used to aid the development of new drugs through the detailed understanding of protein–ligand interactions. In this work, we employed docking simulations to identify potential inhibitors of the *MtSK* from the library of molecules synthesized by the CPBMF, Brazil. The compounds presenting the best binding energy predicted by docking simulations were submitted to in silico prediction of toxicity and hepatotoxicity using the pkCSM [8]. In addition, experiments of binding, enzyme inhibition, and minimal inhibitory concentration (MIC) of in vitro growth of pan-sensitive *Mtb* H37Rv strain were carried out to evaluate the inhibitory potential of ligands selected by the in silico approach. One novel and promising class of inhibitors quinazolin-4(3H)-one was identified. Accordingly, the results here described serve as a basis for further efforts aiming at the rational design of new anti-TB agents targeting the *MtSK* enzyme.

## Methods

### Expression and purification of *MtSK*

For the purification of the recombinant *MtSK* protein, cell growth was performed on a larger scale with the expression condition determined and described by Oliveira et al. [9] with modifications. Briefly, the recombinant plasmid containing the *aroK* gene (pET-23a(+):*aroK*) was used to transform electrocompetent *E. coli* BL21(DE3) cells (Novagen). Transformed cells were selected on LB agar plates containing 50 µg mL<sup>-1</sup> ampicillin. For a pool of cells, 20 colonies from the plate were resuspended in 600 µL of liquid LB medium. After homogenization, 50 µL of this pool were inoculated into 1.5 L of LB medium containing 50 µg mL<sup>-1</sup> ampicillin. After reaching an optical density (OD<sub>600nm</sub>) of 0.4–0.6, the cells were grown at 37 °C in shaker flasks at 180 rpm for a period of 23 h, without IPTG induction. Cells were then collected by centrifugation at 6000×g for 20 min at 4 °C and stored at – 80 °C.

The protein was purified using the ÄKTA purification system (GE HealthCare) through a high-performance liquid chromatography system based on the protocol described by Rosado et al. [10] with modifications. Approximately 6 g of cells were resuspended in 24 mL of 50 mM Tris HCl pH 7.6, disrupted by sonication, and the insoluble fraction removed by centrifugation (18,000 rpm, 30 min, 4 °C). MgCl<sub>2</sub> was added to the supernatant at a final concentration of 40 mM, followed by the addition of 1 mg of DNase under stirring for 30 min at 4 °C and subsequently centrifuged (18,000 rpm, 30 min, 4 °C). The addition of MgCl<sub>2</sub> resulted in the precipitation of the target protein keeping other contaminants

in the supernatant. The precipitate (insoluble fraction) was resuspended in 20 mL of 50 mM Tris HCl 500 mM KCl pH 7.6 and then centrifuged (18,000 rpm, 15 min, 4 °C). To the supernatant, 20 mL of 50 mM Tris HCl 500 mM KCl (NH<sub>4</sub>)<sub>2</sub>SO<sub>4</sub> 2 M pH 7.6 was added, under stirring for 30 min, and then centrifuged (18,000 rpm, 30 min, 4 °C).

The supernatant was loaded onto a hydrophobic interaction column, Phenyl Sepharose 16/10 (GE HealthCare), previously equilibrated with buffer A (50 mM Tris HCl, 500 mM KCl, 1 M (NH<sub>4</sub>)<sub>2</sub>SO<sub>4</sub>, pH 7.6). *MtSK* interacted with the column and eluted in a linear gradient of 10 column volumes containing buffer B (50 mM Tris HCl, 500 mM KCl, pH 7.6), at a flow rate of 1 mL min<sup>-1</sup>. Fractions containing the homogeneous recombinant protein *MtSK* were confirmed by 12% acrylamide gel electrophoresis (SDS-PAGE) stained with Coomassie Brilliant Blue [11]. The protein, after being concentrated using an Amicon ultrafiltration cell (MWCO 10,000 Da), was then centrifuged (18,000 rpm, 30 min, 4 °C), the supernatant was collected, and the concentration was determined by the BCA Kit (BCA Protein Assay Kit).

### Docking procedures

The crystallographic structures of the *MtSK* protein were obtained from the Protein Database (PDB) (<http://www.pdb.org>, accessed on: 24 June 2021). Among the 21 deposited *MtSK* structures, 12 had compounds showing interactions with the SKM substrate active site (PDB Access Codes: 4BQS, 2IYQ, 2IYS, 2IYR, 2G1K, 2IYX, 2IYY, 2IYZ, 2DFN, 1U8A, 1ZYU and 1WE2). For the docking, the following structures were selected: 2IYQ [12] (structure with closed LID, *MtSK*:SKM:ADP complex, 1.80 Å resolution) for its high resolution (< 2 Å) and for its closed conformation, and 2IYS [12] (structure with LID open(A), *MtSK*:SKM complex, 1.40 Å resolution) for being the best resolution among all the deposited crystallographic structures and for containing shikimate in the active site of the structure.

The compounds tested in this work were synthesized by CPBMF from Pontifícia Universidade Católica do Rio Grande do Sul, Brazil. The machine-learning platform pkCSM [8] was used for a preliminary analysis regarding the toxicity of these compounds. A set of 1212 molecules passed through the AMES toxicity filter to select molecules without toxic or hepatotoxic character for the subsequent computer simulations. It is important to note that the compounds were analyzed manually to avoid structure duplication on the platform. From the screening, 298 molecules were selected for docking. The 3D structures of the compounds from the CPBMF database were drawn using Avogadro v1.2.0 program and the protonation states were set according to pH 7.4.

Initially, the re-docking protocol was validated with two crystallographic structures of *MtSK*. The SKM was removed from both structures generating two different conformations: one containing ADP in the active site and the second in the *apo*-form (PDB ID 2IYQ and 2IYS, respectively) [12]. The aim at performing this step was to determine whether the docking algorithm can recover the crystallographic position of the ligand in the active site of the target protein.

The molecules of the chemical library of CPBMF were docked in 2IYQ and 2IYS, using the AutoDock Vina 1.1.2 software compiled to PyRx to identify the ligands with the best binding energies in relation to the target protein [13, 14]. To complete the robustness of the method, the Lamarckian genetic algorithm was assigned, which is a computational approach that provides a set of potential ligand conformations as the principles proposed by Darwin during the molecular adjustment process [15]. The PyRx was used for energy minimization of compounds and to convert all molecules to AutoDock Ligand (PDBQT) format. The established docking protocol was performed as follows: the SK was kept rigid, while the torsional angles of the binder could undergo variations. Water and other compounds used to obtain the crystal were removed from each structure before docking. The 2IYS and 2IYQ structures were used as macromolecules (receptors) [12]. The search space that encompassed the SKM active site was set on a cubic grid, spaced at 0.375 Å, (in both crystallographic structures) with the following dimensions in Å: center (x, y, z) = (36, 36, 30), dimensions (x, y, z) = (15, 15, 15) (PDB: 2IYQ); center (x, y, z) = (15, 20, 33), dimensions (x, y, z) = (15, 15, 15) (PDB: 2IYS). The docking simulation was then run at an exhaustiveness of eight and set to produce a pose ranking (from lowest to highest energy). Subsequently, these ligands were submitted to the PyMOL software (The PyMOL Molecular Graphics System, Version 2.5 Schrödinger, LLC, <https://www.pymol.org>) and Discovery Studio Visualizer program (CDOCKER-Dock, Dassault Systemes BIOVIA, USA) for visual inspection of the poses of potential ligands in the active site of the protein in both conformations.

## Inhibition studies

### Enzymatic assays

The *MtSK* enzyme activity assay was performed in the forward direction by coupling the ADP product to the enzyme pyruvate kinase (PK; EC 2.7.1.40) and lactate dehydrogenase (LDH; EC 1.1.1.27) in a spectrophotometer (UV-2550 UV/Visible, Shimadzu). The NADH-dependent oxidation was monitored continuously at 340 nm ( $\epsilon = 6.22 \times 10^3 \text{ M}^{-1} \text{ cm}^{-1}$ ). The reactions were performed at 25 °C, initiated by the addition of recombinant *MtSK* ( $2 \mu\text{g mL}^{-1}$ ) and monitored for 90 s. The reaction mixture was composed of 100 mM Tris HCl, 100 mM

KCl, 5 mM  $\text{MgCl}_2$  pH 7.6, 1.5 mM PEP, 0.2 mM NADH, 600–100  $\text{U mL}^{-1}$  PK and 900–1400  $\text{U mL}^{-1}$  LDH. The substrates were fixed at  $K_M$ , SKM 650  $\mu\text{M}$  and ATP 112  $\mu\text{M}$  [10]. The ligands were individually added to the reaction mixture at a final concentration of 50  $\mu\text{M}$ , and the final concentration of DMSO that demonstrated not to interfere with the test conditions was 2%.

### Determination of the minimum inhibitory concentration (MIC) in *M. tuberculosis*

The determination of the MIC was performed according to the methodology described by Giacobbo and collaborators [16]. The pan-sensitive *Mtb* H37Rv laboratory strain was used in these studies. The tests were performed in 96-well polystyrene microplates with a “U” shaped bottom. The ligands selected by docking were tested in triplicate for greater reliability of the results. The compounds were solubilized in DMSO and later diluted in Middlebrook 7H9 (7H9) medium containing 10% ADC (albumin, dextrose, and catalase) to a final concentration of 2.5–40  $\mu\text{g mL}^{-1}$ . Serial dilutions of each compound were made directly in the plates. The first-line drug isoniazid (INH) ( $\text{MIC} = 0.31 \mu\text{g mL}^{-1}$ ) was used as a positive control for the experiment. As negative controls, a sterility control of the compounds (without mycobacteria) and a bacterial growth control without the addition of antibiotics (only mycobacterial culture) were used. The mycobacterial strains were cultured in 7H9 medium containing 10% OADC (oleic acid, albumin, dextrose, and catalase) and 0.05% Tween 80, until an  $\text{OD}_{600}$  between 0.8 and 1.0. The cells were then shaken with sterile glass beads (4 mm) for 5 min to break up any existing clumps. The *Mtb* suspensions were divided into aliquots, which were stored at  $-80 \text{ }^\circ\text{C}$ . A 100  $\mu\text{L}$  aliquot of suspension (theoretical  $\text{OD} = 0.006$ ). The final concentration of DMSO in each well is 2.5%. The plates were covered, sealed with parafilm and incubated at 37 °C. After the 7-day incubation period, 60  $\mu\text{L}$  of resazurin solution (0.01%) was added to each well, and the samples incubated for another 48 h [17]. A change in color from blue to pink indicates bacterial growth, and the MIC was defined as the lowest concentration capable of preventing color change. Three tests were performed independently, and the MIC value presented here was the most frequent value among the tests, or the highest value observed among them.

## Results and discussion

### Expression and purification of *MtSK*

Initially, optimizations of the protocols of expression (Fig. S1) and purification of recombinant *MtSK* (Fig. S2 and

S3) allowed efficient protein purification using a two steps protocol comprising a crude extract precipitation followed by a hydrophobic chromatographic step (Phenyl Sepharose 16/10). Protein concentration was determined by the BCA kit and a total of 12.59 mg of *MtSK* was obtained from 9.6 g of cell paste. The enzymatic activity of *MtSK* was assayed in the forward direction by coupling the ADP product to the pyruvate kinase (PK; EC 2.7.1.40) and lactate dehydrogenase (LDH; EC 1.1.1.27) reactions as described elsewhere [10]. The *MtSK*-dependent reduction in NADH concentration was continuously monitored at 340 nm ( $\epsilon = 6.22 \times 10^3 \text{ M}^{-1} \text{ cm}^{-1}$ ), at 25 °C for 90 s of reaction (Fig. 1).

## Docking studies

The first criteria to select compounds of our in-house chemical library were employed to filter out for AMES toxicity and hepatotoxicity. A set of 1212 chemical structures were submitted to the pkCSM platform [8] and 298 molecules passed through the AMES toxicity filter. Although these chemical compounds had not been intentionally developed to bind *MtSK*, it was deemed appropriate to assess whether or not ligands of this enzyme could be identified amongst the chemical library.

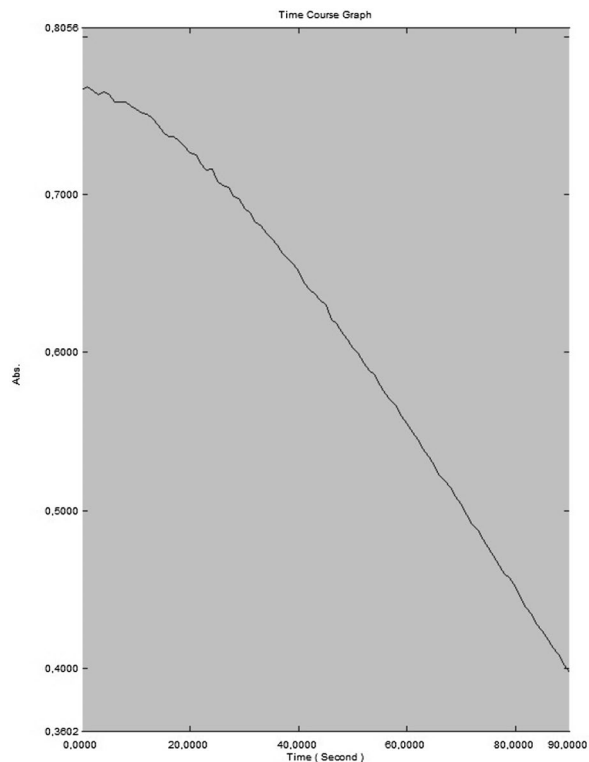


**Fig. 1** Time (seconds) vs absorbance course graph of *MtSK*-dependent reduction in NADH concentration

The AutoDock Vina 1.1.2 implemented in the PyRx [13, 14] software was used for re-docking and docking simulations. The Root Mean Square Deviation (RMSD) value between the ligand presented in the crystal structure and docking pose was 0.77 Å for 2IYS [12] and 0.66 Å for 2IYQ [12] (Fig. 2). This result indicates that the docking simulation was able to reproduce a crystallographic pose and that the protocol is suitable to be used in virtual screening efforts.

The results of docking were evaluated according to the best predicted binding affinity between the two crystallographic structures and these molecules. After fitting simulations and visual analyses, 30 best scoring compounds were selected from the set of 298 compounds. The 30-top candidates of ligands were found to yield strong affinities ranging from  $-8.5$  to  $-9.2$  kcal/mol based on the docking studies, and none of the analyzed 30 compounds showed predicted AMES toxicity or hepatotoxicity (Table 1).

From the visual analysis of the intermolecular interactions in the Discovery Studio Visualizer software, it was possible to observe the potential interaction of the ligands into the shikimate binding cavity. The results showed that the ligand with the highest predicted binding affinity with the enzyme (compound **1a**) participate in van der Waals contact with the Phe57, Gly81 and Pro118 residues in the

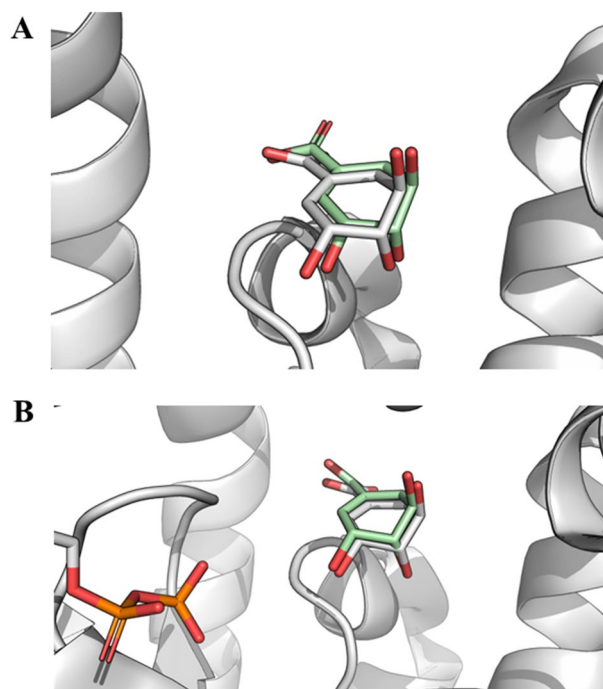


**Fig. 2** Superposition between the crystallographic structure and the best pose generated by the redocking simulations. Redocking using the structures 2IYS (A) and 2IYQ (B). The crystallographic structure is colored by CPK and the carbon atoms of the best poses are colored in green. Image generated with PyMOL

**Table 1** Top 30 compounds obtained from docking

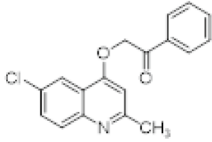
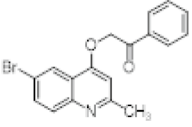
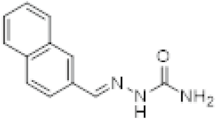
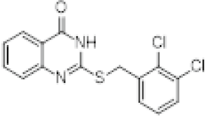
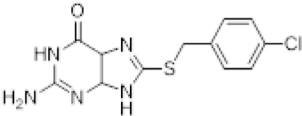
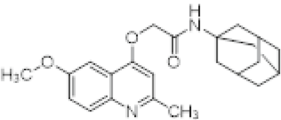
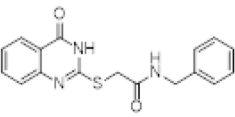
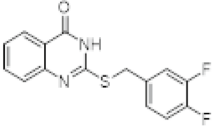
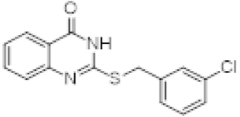
Compound ID	Chemical name	Chemical structure	Binding energy (kcal/mol)
1a	2-((6-Chloro-2-methylquinolin-4-yl)oxy)-1-phenylethan-1-one		-9.2
1b	2-((6-Bromo-2-methylquinolin-4-yl)oxy)-1-phenylethan-1-one		-9.1
1c	( <i>E</i> )-2-(Naphthalen-2-ylmethylene)hydrazine-1-carboxamide		-8.9
2a	2-((2,3-Dichlorobenzyl)thio)quinazolin-4(3H)-one		-8.9
2b	2-Amino-8-((4-chlorobenzyl)thio)-1,4,5,9-tetrahydro-6H-purin-6-one		-8.9
2c	<i>N</i> -(Adamantan-1-yl)-2-((6-methoxy-2-methylquinolin-4-yl)oxy)acetamide		-8.8
3a	<i>N</i> -Benzyl-2-((4-oxo-3,4-dihydroquinazolin-2-yl)thio)acetamide		-8.8
3b	2-((3,4-Difluorobenzyl)thio)quinazolin-4(3H)-one		-8.8
3c	2-((3-Chlorobenzyl)thio)quinazolin-4(3H)-one		-8.7

Table 1 (continued)

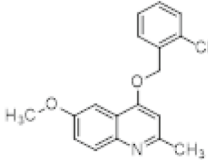
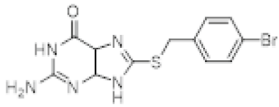
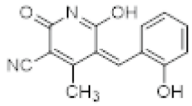
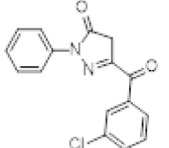
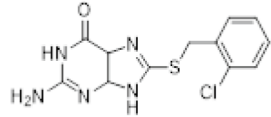
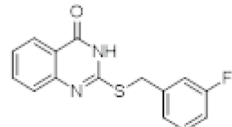
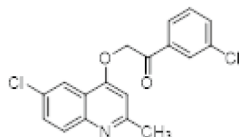
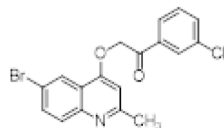
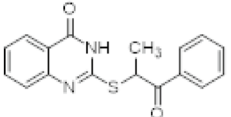
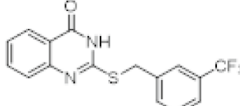
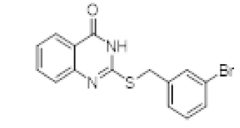
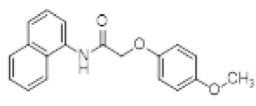
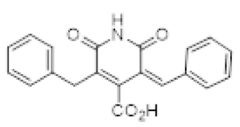
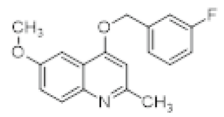
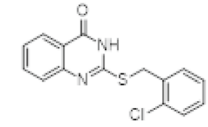
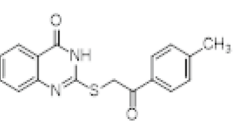
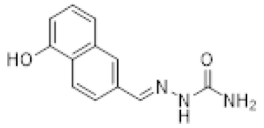
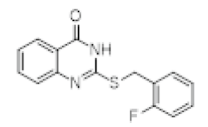
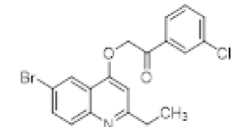
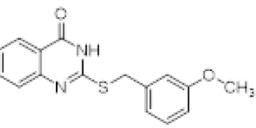
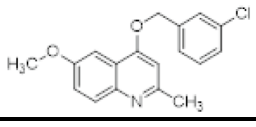
3d	4-((2-Chlorobenzyl)oxy)-6-methoxy-2-methylquinoline		-8.7
3e	2-Amino-8-((4-bromobenzyl)thio)-1,4,5,9-tetrahydro-6H-purin-6-one		-8.7
4a	(Z)-6-Hydroxy-5-(2-hydroxybenzylidene)-4-methyl-2-oxo-2,5-dihydropyridine-3-carbonitrile		-8.7
4b	5-(3-Chlorobenzoyl)-2-phenyl-2,4-dihydro-3H-pyrazol-3-one		-8.7
5a	2-Amino-8-((2-chlorobenzyl)thio)-1,4,5,9-tetrahydro-6H-purin-6-one		-8.6
5b	2-((3-Fluorobenzyl)thio)quinazolin-4(3H)-one		-8.6
5c	2-((6-Chloro-2-methylquinolin-4-yl)oxy)-1-(3-chlorophenyl)ethan-1-one		-8.6
5d	2-((6-Bromo-2-methylquinolin-4-yl)oxy)-1-(3-chlorophenyl)ethan-1-one		-8.6
6a	2-((1-Oxo-1-phenylpropan-2-yl)thio)quinazolin-4(3H)-one		-8.6
6b	2-((3-(Trifluoromethyl)benzyl)thio)quinazolin-4(3H)-one		-8.6

Table 1 (continued)

6c	2-((3-Bromobenzyl)thio)quinazolin-4(3 <i>H</i> )-one		-8.6
6d	2-(4-Methoxyphenoxy)-N-(naphthalen-1-yl)acetamide		-8.6
7a	( <i>Z</i> )-5-Benzyl-3-benzylidene-2,6-dioxo-1,2,3,6-tetrahydropyridine-4-carboxylic acid		-8.5
7b	4-((3-Fluorobenzyl)oxy)-6-methoxy-2-methylquinoline		-8.5
7c	2-((2-Chlorobenzyl)thio)quinazolin-4(3 <i>H</i> )-one		-8.5
7d	2-((2-Oxo-2-(p-tolyl)ethyl)thio)quinazolin-4(3 <i>H</i> )-one		-8.5
8a	( <i>E</i> )-2-((5-Hydroxynaphthalen-2-yl)methylene)hydrazine-1-carboxamide		-8.5
8b	2-((2-Fluorobenzyl)thio)quinazolin-4(3 <i>H</i> )-one		-8.5
8c	2-((6-Bromo-2-ethylquinolin-4-yl)oxy)-(3-chlorophenyl)ethan-1-one		-8.5
8d	2-((3-Methoxybenzyl)thio)quinazolin-4(3 <i>H</i> )-one		-8.5
8e	4-((3-Chlorobenzyl)oxy)-6-methoxy-2-methylquinoline		-8.5

shikimate binding cavity and makes a hydrogen bond with the Arg58 (Fig. 3) [18–20].

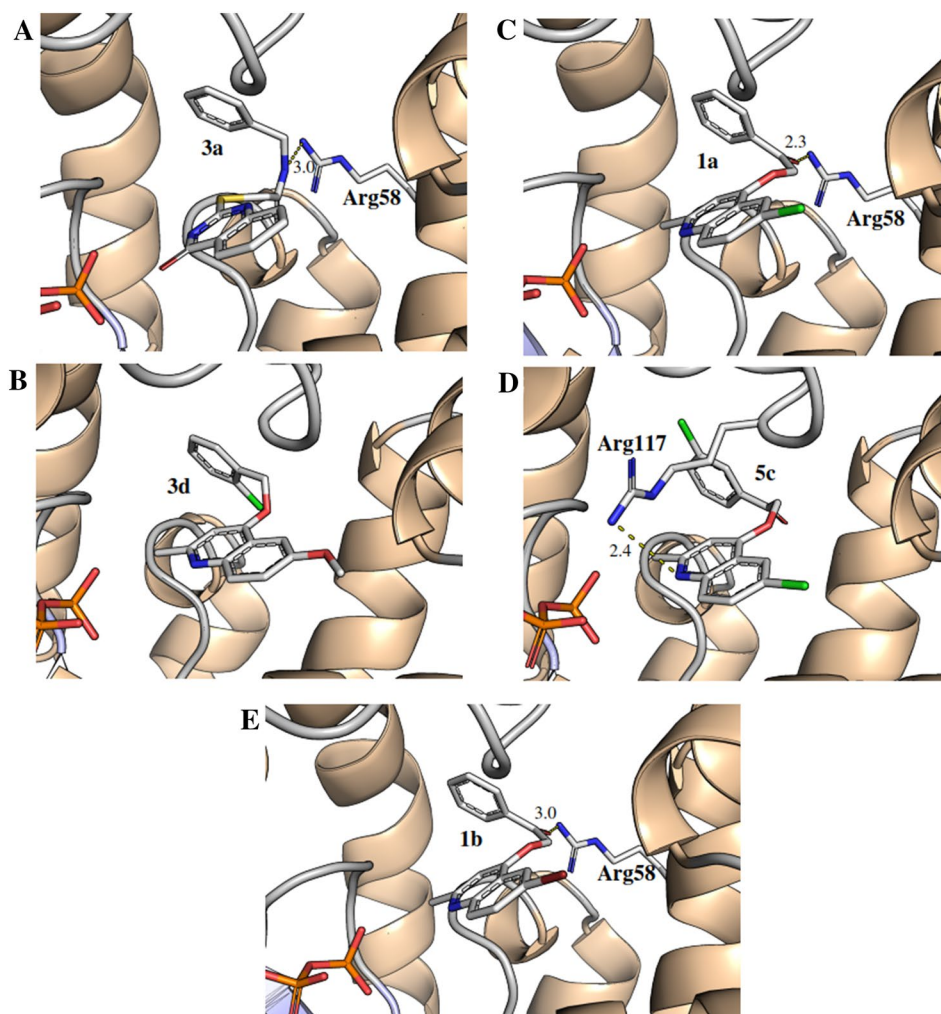
The knowledge of the amino acids residues involved in the protein:ligand interaction of the shikimate binding cavity highlights potential ligands with high binding affinity to this site and point to candidates for inhibitors. Furthermore, the residues that establish these molecular interactions are fundamental to the reaction catalyzed by the enzyme. The residues Arg58, Arg136 and Gly80 have been shown to participate in intermolecular hydrogen bonds with the shikimate in this substrate-binding pocket [7]. On the other hand, the residues Ile45, Asp34, Pro11, Pro118, Gly79, Phe57, Leu119 and Gly81 make van der Waals contacts with shikimate [21]. By analyzing the potential ligands ranked by the binding energy, it is possible to observe essential residues that enable the binding of the ligand to the active site of the *MtSK* enzyme, especially hydrogens bonds and van der Waals contacts. After this analysis, the ligands with the best binding energy scores were submitted to in vitro characterization and validation analyses.

## Inhibition studies

### Screening of compounds as potential inhibitors

Initially, the 30 compounds selected for experimental analysis were evaluated for formation of precipitates to evaluate the maximum concentration allowed by the solubility. After this test, thirteen (13) compounds showed limited solubility in the buffer mixture and were thus removed from enzyme inhibition screening as no reliable results could be obtained. Therefore, seventeen compounds were analyzed for their inhibition of *MtSK* enzyme activity. We evaluated the possibility of inhibition of these compounds through the coupled assay of Pyruvate kinase (PK) and Lactate dehydrogenase (LDH) for the activity of *MtSK*. The spectrophotometer experiment evaluates the activity of *MtSK*, being monitored by the dependent oxidation of NADH at 340 nm [10]. Through this screening approach, we identified a total of 11 compounds that showed inhibition of the *MtSK*-catalyzed chemical reaction at final fixed concentration of 50  $\mu\text{M}$ . These results are given in Table 2.

**Fig. 3** Predicted docking orientations of **3a** (a), **3d** (b), **1a** (c), **5c** (d) e **1b** (e) into the binding pocket of *MtSK* (PDB ID: 2IYQ)





The 3,4-difluorobenzyl **3b** and 3-chlorobenzyl derivatives **3c** proved to be the most potent inhibitors (23.83 and 22.11%, respectively), and both belong to the chemical class quinazolin-4(3*H*)-one. In compound **3b** there is the presence of halogen fluorine (difluorobenzyl) and in **3c** there is chlorine (chlorobenzyl). These halogen atoms that have long been used for hit-to-lead or lead-to-drug conversions [22]. Halogens (F, Cl, and Br) are usually employed as univalent isosteres to study the effect of increasing volume and polarizability on ligand interactions to a target, thereby probing the role played by van der Waals forces. Accordingly, compounds containing chlorine and fluorine substituents at different positions on the aromatic ring were also tested to evaluate whether or not the positioning and identity of halogens would improve the inhibitory activity of *MtSK* (Table 3). The 3,4-difluorobenzyl compound (**3b**), 3-fluorobenzyl (**5b**), 6-fluorobenzyl (**8b**) and 4-fluorobenzyl (**9a**) were thus tested. The difluorobenzyl (**3b**) showed to be a better inhibitor as compared to any fluorobenzyl (**5b**, **8b**, **9a**) or benzyl (**9b**) quinazolin-4(3*H*)-one compound (Table 3). These data suggest that the presence of fluorine substituents at both the *meta* and *para* positions of the benzene ring are required for improved inhibitory activity. The chlorine-containing compounds showed a different pattern. No improvement of inhibitory activity as compared to the 3-chlorobenzyl compound (**3c**) could be achieved as the 4-chlorobenzyl

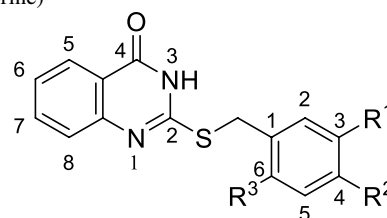
**Table 2** In vitro inhibitory activities observed on the reaction catalyzed by *MtSK*

Compound	Inhibitory activity (%) <sup>a</sup>
1a	5.34
1b	8.03
1c	1.32
3a	5.76
3b	23.83
3c	22.11
3d	8.42
3e	1.17
5a	–
5b	2.82
5c	2.15
6a	–
6d	–
7b	–
8a	0.39
8b	–
8e	–

<sup>a</sup>Assigned at compounds final 50  $\mu$ M concentrations in assay mixture

– Non-detected inhibitory activity

**Table 3** In vitro inhibitory activities observed on the reaction catalyzed by *MtSK* between compounds with substituent halogens (chlorine and fluorine)



Compound	R <sup>1</sup>	R <sup>2</sup>	R <sup>3</sup>	Inhibitory activity (%) <sup>a</sup>
3b	F	F	H	23.83
5b	F	H	H	2.82
8b	H	H	F	–
9a	H	F	H	–
9b	H	H	H	–
3c	Cl	H	H	22.11
9c	H	Cl	H	10.11
9d	Cl	Cl	H	11.46
9e	H	H	Cl	–

<sup>a</sup>Assigned with 50  $\mu$ M final fixed concentrations of compounds in assay mixtures

– Non-detected inhibitory activity

(**9c**), 3,4-chlorobenzyl (**9d**) and 6-chlorobenzyl (**9e**) were assayed (Table 3). The results also suggest that halogen substitution at the *ortho* position of benzene ring (**8b**, **9e**) is deleterious to inhibitory activity (Table 3). A comparison between 3-fluorobenzyl (**5b**) and 3-chlorobenzyl compound (**3c**) indicate that halogen bond formation may play a role in target interaction as chlorine tend to have greater extent of charge separation and larger  $\delta$ -hole as compared to fluorine [22]. However, these conclusions should be considered with caution as they are based on a single concentration of compounds, and further experimental data are needed to provide a more solid basis on which to draw structure–activity relationships.

The in silico protocol (dry-lab) here presented aimed at identifying ligands and whether or not they prove to be inhibitors had to be evaluated by biochemical analysis (wet-lab). At any rate, the results here presented show that the computational approach employed could identify ligands and a limited number of inhibitors of *MtSK* from a fairly small library of chemical compounds, which represents a notable achievement. It is envisioned that this in silico approach should be employed in the near future to screen much larger libraries of chemical compounds, ideally, comprised of scaffolds encompassing a greater chemical space.

### Determination of the minimum inhibitory concentration (MIC) in *Mtb*

A chemical compound that showed no inhibition of *MtSK* activity could, however, prove to be effective as inhibitor of in vitro growth of the pan-sensitive *Mtb* H37Rv strain. Hence, MIC values, defined as the lowest concentration of each compound that was able to inhibit visible growth in 96-well plates, were determined for 22 compounds, in triplicate, with isoniazid as a positive control. Interestingly, compounds **1a**, **1b**, **3d** and **5c** that had shown a negligible effect on enzyme inhibition compared to ortho, for the compound 3,4-difluorobenzyl (**3b**) and *meta* monosubstituted chlorine benzyl (**3c**) (Table 3), were active against *Mtb*, showing MIC values of 16  $\mu\text{M}$ , 14  $\mu\text{M}$ , 18.83  $\mu\text{M}$  and 7.2  $\mu\text{M}$ , respectively (Table 4) (Fig. 1). However, whether *MtSK* is the intracellular target of these compounds will have to await further experimental data. The compounds **3a** and **7b** showed the lowest MIC values of, respectively, 4.79  $\mu\text{M}$  and 5  $\mu\text{M}$  (Table 4). It should be pointed out that the MIC values for compounds **3a** and **3d** had been reported elsewhere [23, 24]. Compound **7b** showed inhibitory activity of in vitro growth of *Mtb* H37Rv strain (Table 4) and no inhibition of *MtSK* enzyme activity (Table 2). This result raises the possibility of alternative targets for this compound that will be pursued in future efforts. The compounds **1c**, **3b**, **3c**, **3e**, **5a**, **5b**, **6a**, **6d**, **8a**, **8b**, **8e**, **9a**, **9b**, **9c**, **9d** and **9e**, which showed no inhibitory effect against *MtSK* (Table 3), were not able to inhibit the mycobacterial growth at the limit of their solubility (Table 4).

### Conclusion

In this study, an in-house chemical library containing different chemical classes was employed to evaluate its binding and inhibition profile against the *MtSK* enzyme. Computational methodologies were used to evaluate the toxicity/hepatotoxicity of the molecules and to probe the intermolecular interactions of these compounds in the active site of the enzyme. Biochemical assays were used to provide experimental evidence for in silico predictions such as enzyme inhibition and MIC measurements. The results obtained by the computational methodology were in fairly good agreement with the experimental data, demonstrating that from 1212 compounds it was possible to identify compounds that inhibit both *MtSK* and the in vitro growth of *Mtb* (compounds **1a**, **1b**, **3a**, **3d** and **5c**), or showed no enzyme inhibition but was active against mycobacterial growth (e.g. **7b**). The chemical class of quinazoline-4(3*H*)-one compounds revealed a promising scaffold for *MtSK* enzyme inhibitor optimization efforts but limited potential for anti-TB drug development as it did not inhibited mycobacteria. An

**Table 4** Antimicrobial evaluation of 22 compounds against the in vitro growth of pan-sensitive H37Rv strain of *M. tuberculosis*

Compound ID	MIC ( $\mu\text{M}$ )
1a	16
1b	14
1c	–
3a*	4.79
3b	–
3c	–
3d*	18.83
3e	–
5a	–
5b	–
5c	7.2
6a	–
6d	–
7b	5
8a	–
8b	–
8e	–
9a	–
9b	–
9c	–
9d	–
9e	–

\*Data has been published previously

– Non-detected inhibitory activity

improved protein expression and purification protocol has also been established, which should aid in efforts to screen for inhibitors of *MtSK* enzyme activity. For example, structural modifications of compounds **1a**, **1b**, **3a**, **3d** and **5c** can be sought to optimize their inhibitory activity against the *MtSK* enzyme and *Mtb* growth.

**Supplementary Information** The online version contains supplementary material available at <https://doi.org/10.1007/s10822-022-00495-w>.

**Acknowledgements** This work was supported by National Institute of Science and Technology on Tuberculosis (Decit/SCTIE/MS-MCT-CNPq-FNDTC-CAPES-FAPERGS) [Grant Number 421703/2017-2], Banco Nacional de Desenvolvimento Econômico e Social (BNDES/FUNTEC) [Grant Number 14.2.0914.1] and FAPERGS [Grant Number 19/1724-3 PQG]. L.A.B. (CNPq, Grant 303499/2021-4), C.V.B. (CNPq, Grant 311949/2019-3) and P.M. (CNPq, Grant 305203/2018-5) are Research Career Awardees of CNPq. This study was financed in part by the Coordenação de Aperfeiçoamento de Pessoal de Nível Superior-Brasil (CAPES), Finance Code 001.

**Author contributions** TFF, LAB, LFSMT and CDR wrote the manuscript. TFF, LAB and CDR planned the in vitro experiments. TFF and CDR carried out the in vitro experiments. TFF and LFSMT planned the in silico experiments and carried out the simulations. TFF, LAB, LFSMT, CDR, CVB and PM contributed to the interpretation of the

results. AFB and PM synthesized the compounds. BLA, FSMH, MAP and AMC designed and performed the Minimum Inhibitory Concentration (MIC) experiments and analyzed the data. LFSMT prepared the Fig. 1. EVS carried out the implementation of computer models to facilitate the analysis of in silico data. All authors reviewed the manuscript.

**Funding** This work was supported by National Institute of Science and Technology on Tuberculosis (Decit/SCTIE/MS-MCT-CNPq-FNDTC-CAPES-FAPERGS) [Grant Number 421703/2017-2], Banco Nacional de Desenvolvimento Econômico e Social (BNDES/FUNTEC) [Grant Number 14.2.0914.1] and FAPERGS [Grant Number 19/1724-3 PQG]. L.A.B. (CNPq, Grant 303499/2021-4), C.V.B. (CNPq, Grant 311949/2019-3) and P.M. (CNPq, Grant 305203/2018-5) are Research Career Awardees of CNPq. This study was financed in part by the Coordenação de Aperfeiçoamento de Pessoal de Nível Superior-Brasil (CAPES), Finance Code 001.

**Data availability** The protein–ligand complexes generated during the current study are available from the corresponding author on reasonable request.

## Declarations

**Conflict of interest** There are no conflict to declare.

## References

- World Health Organization, Global tuberculosis report (2021) WHO Press, Geneva <https://www.who.int/publications/i/item/9789240037021> Accessed 13 Jun 2022
- Ducati RG, Basso LA, Santos DS (2007) *Curr Drug Targets* 8:423–435
- Parish T, Stoker NG (2002) *Microbiology* 148:3069–3077
- Yan H, Tsai M (1999) *Adv Enzymol Relat Areas Mol Biol* 73:103–134
- Vonrhein C, Schlauderer GJ, Schulz GE (1995) *Structure* 3:483–490
- Coracini JD, Azevedo WF Jr (2014) *Curr Med Chem* 21:592–604
- Pereira JH, de Oliveira JS, Canduri F, Dias MVB, Palma MS, Basso LA, Azevedo WF Jr (2004) *Acta Crystallogr Sect D: Biol Crystallogr* 60(Pt 12 Pt 2):2310–2319
- Pires DEV, Blundell TL, Ascher DB (2015) *J Med Chem* 58(9):4066–4072
- Oliveira JS, Pinto CA, Basso LA, Santos DS (2001) *Protein Expr Purif* 22:430–435
- Rosado LA, Vasconcelos IB, Palma MS, Frappier V, Najmanovich J, Santos DS, Basso LA (2013) *PLoS ONE* 8(5):e61918
- Laemmli UK (1970) *Nature* 227:680–685
- Hartmann MD, Bourenkov GP, Strizhov AON, Bartunik HD (2006) *J Mol Biol* 364:411–423
- Trott O, Olson AJ (2010) *J Comput Chem* 31:455–461
- Dallakyan S, Olson AJ (2015) *Methods Mol Biol* 1263:243–250
- Fuhrmann J, Rurainski A, Lenhof HP, Neumann D (2010) *J Comput Chem* 31:1911–1918
- Giacobbo BC, Pissinate K, Rodrigues-Junior V, Villela AD, Grams ES, Abadi BL, Subtil FT, Sperotto N, Trindade RV, Back DF, Campos MM, Basso LA, Machado P, Santos DS (2017) *Eur J Med Chem* 126:491–501
- Palomino JC, Martin A, Camacho M, Guerra H, Jean S, Portaels F (2002) *Antimicrob Agents Chemother* 46:2720
- Simithy J, Fuanta NR, Alturki M, Hobrath JV, Wahba AE, Pina I, Rath J, Hamann MT, DeRuiter J, Goodwin DC, Calderón AI (2018) *Biochemistry* 57:4923–4933
- Simithy J, Fuantab NR, Hobrath JV, Kochanowska-Karamyan A, Hamann MT, Goodwin DC, Calderón AI (2018) *BBA—Proteomics* 1866:731–739
- Kumar M, Verma S, Sharma S, Srinivasan A, Sing TP, Kaur P (2010) *Chem Biol Drug Des* 76:277–284
- Vianna CP, Azevedo WF Jr (2012) *J Mol Model* 18:755–764
- Sirimulla S, Bailey JB, Vegesna R, Narayan M (2013) *J Chem Inf Model* 53(11):2781–2791
- Macchi FS, Pissinate K, Villela AD, Abadi BL, Rodrigues-Junior V, Nabinger DD, Altenhofen S, Sperotto N, Dadda AS, Subtil FT, de Freitas TF, Rauber APE, Borsoi AF, Bonan CD, Bizarro CV, Basso LA, Santos DS, Machado P (2018) *Eur J Med Chem* 155:153–164
- Borsoi AF, Paz JD, Abadi BL, Macchi FS, Sperotto N, Pissinate K, Rambo RS, Ramos AS, Machado D, Viveiros M, Bizarro CV, Basso LA, Machado P (2020) *Eur J Med Chem* 192:112179

**Publisher's Note** Springer Nature remains neutral with regard to jurisdictional claims in published maps and institutional affiliations.

Springer Nature or its licensor (e.g. a society or other partner) holds exclusive rights to this article under a publishing agreement with the author(s) or other rightsholder(s); author self-archiving of the accepted manuscript version of this article is solely governed by the terms of such publishing agreement and applicable law.

## Authors and Affiliations

Talita Freitas de Freitas<sup>1,2</sup> · Candida Deves Roth<sup>1</sup> · Bruno Lopes Abadi<sup>1</sup> · Fernanda Souza Macchi Hopf<sup>1,3</sup> · Marcia Alberton Perelló<sup>1</sup> · Alexia de Matos Czczot<sup>1,2</sup> · Eduardo Vieira de Souza<sup>1,3</sup> · Ana Flávia Borsoi<sup>1,2</sup> · Pablo Machado<sup>1,2,3</sup> · Cristiano Valim Bizarro<sup>1,3</sup> · Luiz Augusto Basso<sup>1,2,3</sup> · Luis Fernando Saraiva Macedo Timmers<sup>1,4,5,6</sup>

<sup>1</sup> Centro de Pesquisas em Biologia Molecular e Funcional (CPBMF), Instituto Nacional de Ciência e Tecnologia em Tuberculose (INCT-TB), Pontifícia Universidade Católica do Rio Grande do Sul (PUCRS), Porto Alegre, Brazil

<sup>2</sup> Programa de Pós-Graduação em Medicina e Ciências da Saúde, Pontifícia Universidade Católica do Rio Grande do Sul, Porto Alegre, Rio Grande do Sul 90616-900, Brazil

<sup>3</sup> Programa de Pós-Graduação em Biologia Celular e Molecular, Pontifícia Universidade Católica do Rio Grande do Sul, Porto Alegre, Rio Grande do Sul 90616-900, Brazil

<sup>4</sup> Universidade do Vale do Taquari (Univates), Lajeado, Rio Grande do Sul 95914-014, Brazil

<sup>5</sup> Programa de Pós-Graduação em Biotecnologia,  
Universidade do Vale do Taquari (Univates), Lajeado,  
Rio Grande do Sul 95914-014, Brazil

<sup>6</sup> Programa de Pós-Graduação em Ciências Médicas,  
Universidade do Vale do Taquari (Univates), Lajeado,  
Rio Grande do Sul 95914-014, Brazil